

This is a repository copy of *In situ mechanical and molecular investigations of collagen/apatite biomimetic composites combining Raman spectroscopy and stress-strain analysis*.

White Rose Research Online URL for this paper:

<https://eprints.whiterose.ac.uk/106191/>

Version: Published Version

Article:

Chatzipanagis, Konstantinos, Baumann, Christoph George orcid.org/0000-0002-8818-972X, Sandri, Monica et al. (3 more authors) (2016) In situ mechanical and molecular investigations of collagen/apatite biomimetic composites combining Raman spectroscopy and stress-strain analysis. *Acta Biomaterialia*. ISSN 1742-7061

<https://doi.org/10.1016/j.actbio.2016.09.028>

Reuse

This article is distributed under the terms of the Creative Commons Attribution (CC BY) licence. This licence allows you to distribute, remix, tweak, and build upon the work, even commercially, as long as you credit the authors for the original work. More information and the full terms of the licence here:

<https://creativecommons.org/licenses/>

Takedown

If you consider content in White Rose Research Online to be in breach of UK law, please notify us by emailing eprints@whiterose.ac.uk including the URL of the record and the reason for the withdrawal request.



Contents lists available at ScienceDirect

Acta Biomaterialia

journal homepage: www.elsevier.com/locate/actabiomat

Full length article

In situ mechanical and molecular investigations of collagen/apatite biomimetic composites combining Raman spectroscopy and stress-strain analysis

Konstantinos Chatzipanagis^a, Christoph G. Baumann^b, Monica Sandri^c, Simone Sprio^c, Anna Tampieri^c, Roland Kröger^{a,*}^a Department of Physics, University of York, York, United Kingdom^b Department of Biology, University of York, York, United Kingdom^c Institute of Science and Technology for Ceramics, National Research Council, Faenza, Italy

ARTICLE INFO

Article history:

Received 5 April 2016

Received in revised form 14 September 2016

Accepted 22 September 2016

Available online xxxx

Keywords:

Raman spectroscopy

Collagen

Apatite

Biomaterialization

Tensile stress

ABSTRACT

We report the design, fabrication and application of a novel micro-electromechanical device coupled to a confocal Raman microscope that enables *in situ* molecular investigations of micro-fibers under uniaxial tensile load. This device allows for the mechanical study of micro-fibers with diameters in the range between 10 and 100 μm and lengths of several hundred micrometers. By exerting forces in the mN range, the device enables an important force range to be accessed between that of atomic force microscopy and macroscopic stress-strain measurement devices. The load is varied using a stiffness-calibrated glass micro-needle driven by a piezo-translator during simultaneous Raman microscopy imaging. The method enables experiments probing the molecular response of micro-fibers to external stress. This set-up was applied to biomimetic non-mineralized and mineralized collagen micro-fibers revealing that above 30% mineralization the proline-related Raman band shows a pronounced response to stress, which is not observed in non-mineralized collagen. This molecular response coincides with a strong increase in the Young's modulus from 0.5 to 6 GPa for 0% and 70% mineralized collagen, respectively. Our results are consistent with a progressive interlocking of the collagen triple-helices by apatite nanocrystals as the degree of mineralization increases.

Statement of Significance

Collagen and apatite are the main constituents regulating the mechanical properties of bone. Hence, an improved understanding of the impact of mineralization on these properties is of large interest for the scientific community. This paper presents systematic studies of synthetic collagen microfibers with increasing apatite content and their response to tensile stress by using a novel self-made electromechanical device combined with a Raman spectrometer for molecular level studies. The impact of apatite on the mechanical and molecular response of collagen is evaluated giving important insights into the interaction between the mineral and organic phases. Therefore our findings expand the fundamental understanding of the mechanics of the apatite/collagen system relevant for the design of bio-composites with similar bio-mimicking properties for e.g. bone regrowth in medical applications.

© 2016 Published by Elsevier Ltd on behalf of Acta Materialia Inc.

1. Introduction

Understanding the link between the mechanical and the molecular properties of micro-fibrillar materials is of great importance for the design of hard-soft matter composites such as collagen/

apatite micro-fibers for biomedical applications, e.g. as growth templates for bone formation [1,2]. This is crucial for the controlled realization of composites with desired mechanical properties and optimized fracture toughness and Young's modulus.

In this context combining Raman microscopy with *in situ* stress-strain measurements is a powerful means to investigate the molecular response of materials to external tensile stress. Currently available commercial devices only allow for the study of bulk

* Corresponding author.

E-mail address: roland.kroger@york.ac.uk (R. Kröger).

materials (dimensions of several hundred micrometers and above), which – as in the case of bone or mineralized tendon – have a complex three-dimensional microstructure where individual constituents at various hierarchical levels can contribute to the bulk mechanical properties [2–5]. This limitation prevents a direct interpretation of the obtained data since stress relief occurs along convoluted pathways due to the three-dimensional nature of the sample. Alternatively, atomic force microscopy (AFM) can be applied to study micro-fibers on the nanometer scale [6]. However, AFM on its own does not provide information on the molecular response to stress. These restrictions motivate our approach to design a dedicated stage for Raman-microscopy enabling the investigation of micro-fibers with bespoke glass micro-needles to apply calibrated forces in the mN range required for material systems such as mineralized collagen. This is motivated by the fact that the Young's modulus of collagen is of the order of hundreds of MPa and hence micro-fibers with diameters of 100 μm and below require external forces of the order of mN to obtain observable extension upon loading. Our research is driven by the interest in novel collagen/apatite composites as potential templates for implant overgrowth by bone [7] motivating our focus on collagen-based micro-fibers.

2. Collagen micro-fibers and Raman microscopy

Collagen is the most abundant fibrous protein found in the human body and other vertebrates [8]. It is the main building block of connective tissues such as skin and tendon as well as bone and teeth and consists of amino acid sequences arranged in a characteristic triplet (Gly–Pro–Hyp), where glycine (Gly), proline (Pro) and hydroxyl-proline (Hyp) constitute almost 30% of the polypeptide chain [8,9]. Type I collagen, as studied in our work, is assembled in a hierarchical fashion by a twisted left-handed helix, three of which can assemble into a right-handed super-helix forming the collagen molecule known as tropo-collagen. Single tropo-collagen molecules have a length of typically 300 nm and a diameter of 1.5 nm. The triple helices assemble in a staggered manner to form collagen fibrils with diameters of approximately 100 nm [10–12]. These fibrils tend to form extended micro-fibers on which our work concentrates. Hard apatite (Ap) deposited in conjunction with the soft collagen is a key component of bone, which in turn is a three-dimensional hierarchical bio-composite giving rise to the remarkable combination of fracture toughness and hardness in bone. Comprehending the correlation between mechanical properties and molecular structure requires a deeper understanding of the way in which this complex material responds to external forces and how it accommodates mechanical stress. Consequently, a wide range of techniques has been employed in the past decades to investigate the mechanical behavior of various biomaterials with particular focus on the tensile properties of fibrous materials with characteristic diameters ranging from the mm to the nm scale using different devices for mechanical testing.

Raman spectroscopy is a powerful tool for the study of the molecular structure of materials [13]. It is particularly useful for the investigation of water-containing bio-composites, since it does not suffer from the associated strong absorption observed in other types of spectroscopy, e.g. in FTIR [13]. Furthermore, it does not require large amounts of material or specific labelling of the sample. This is particularly important when combined with *in situ* stress-strain measurements as presented in this work. Collagen is an extensively studied biomaterial regarding its mechanical properties and various types of commercial or custom-built devices have been used for mechanical measurements [14,15]. Eppel et al. [16] studied the mechanical properties

of single collagen fibrils under tensile stress using a custom-built micro-electromechanical device that allowed the use of immunofluorescence microscopy to image the fibrils. This is useful when measuring strain values and structural changes on the microscale, while nano-indentation was applied on single fibrils using an AFM tip [17]. Furthermore, AFM was used to exert tensile stress on collagen fibrils extracted from red deer antler with different levels of mineral content ranging from 30% to 60% for investigation of their mechanical response [6]. Other commercially available devices combined with Raman spectroscopy were also employed for *in situ* molecular investigations of the mechanical properties of pig-tail tendon [18] and human skin [19].

To the best of our knowledge, there has not been a systematic *in situ* Raman spectroscopy investigation of collagen micro-fibers as a function of calibrated mechanical loading for different degrees of mineralization. Studying micro-fibers rather than bulk specimens is important since hierarchical bio-composites such as bone or tendon will anisotropically respond to stress. Hence, the strain distribution strongly depends on the internal structure of the sample. This renders a decomposition of the different contributions to the stress-response (e.g. molecular stretching/bending and relaxation via alignment) difficult, if not impossible. Micro-fibrous samples can be uniaxially stretched reducing the possible pathways for stress-relaxation to molecular stretching and bending as well as inter-fibrillar glide. Our technique enables mechanical manipulation of micro-fibers on a length-scale between that accessible using AFM (maximum extensions <10 μm) and standard macroscale mechanical testing tools. Hence, this technique combined with *in situ* Raman spectroscopy can provide key insight into the correlation between the molecular structure of micro-fibers and their mechanical properties.

2.1. Experimental details

Our custom-built electromechanical device was designed to be compatible with a commercial Raman microscope for *in situ* studies. The unique characteristics of this device can be summarized as follows: i) it is possible to conduct Raman spectroscopy on a micro-fiber while simultaneously applying tensile load for *in situ* molecular investigations of structural changes accompanying mechanical deformation, ii) the load can be repeatedly applied and removed by displacing the calibrated micro-needle with a piezo-translator (PZT) to follow elastic or plastic deformation, iii) bespoke micro-needles with different fine tip lengths and/or diameters can be produced to provide spring constants of an appropriate magnitude for applying mechanical stress to micro-fibers. This device combined with Raman microscopy allows for the study of the molecular response of both mineralized and non-mineralized collagen under tensile stress, and for the investigation of how increases in collagen mineralization affect its mechanical properties. Fig. 1a and b show a schematic and a photographic representation of the setup integrated into a stainless steel case for mechanical stability and environmental control. The central elements of the micromechanical manipulator are two glass micro-needles with different stiffness values – a rigid needle is fixed to one end of the micro-fiber while a flexible needle attached to the opposite end of the micro-fiber acts as the calibrated force transducer. The flexible needle is mounted to a PZT and is calibrated gravimetrically using a set of defined weights. The flexible micro-needle can be uniaxially displaced by the PZT over a range of up to 450 μm , resulting in a calibrated force being applied reversibly to the micro-fiber. The static micro-needle attached at the opposite end of the micro-fiber must not bend during the micromanipulation experiment. This can be achieved by using a static micro-needle with approximately half the length and twice the diameter of the flexible micro-needle. Furthermore,

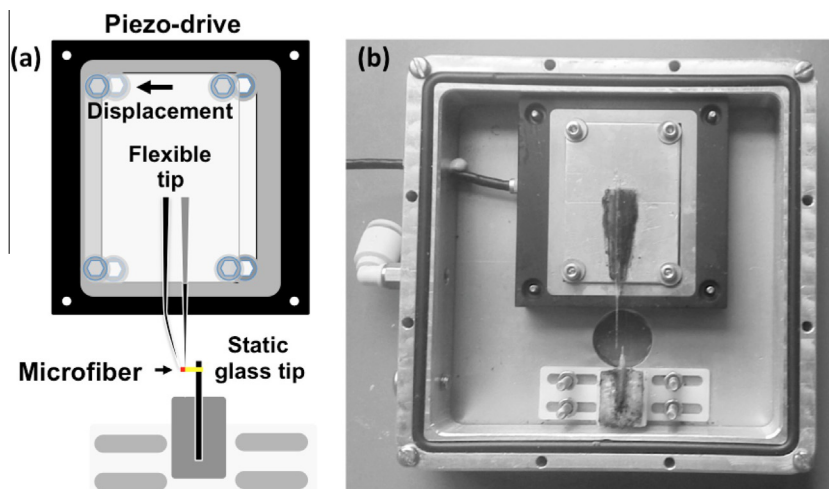


Fig. 1. (a) Schematic view of the stress-strain device showing the key components. The calibrated flexible needle is attached to the piezo drive and the static glass tip is mounted to a stable support. The calibrated needle is displaced using the piezo drive exerting uniaxial stress. (b) Image of the stress-strain testing device. The side length of the casing is 11.5 cm.

it is a requirement that the flexible micro-needle acts elastically upon deflection following Hooke's law. The spring constant of the flexible micro-needle is chosen such that the resulting force applied to the micro-fiber is sufficient to observe a tensile response in the mN range. In this set-up, the micro-fibers are attached to both tips using crystal bond (SPI Supplies Inc.) and the displacement of the PZT (PI MikroMove, PI 2.4.0) is computer-controlled.

Potential laser-induced chemical modification of the sample during Raman microscopy was probed by acquiring spectra as a function of time at a single spot on a static micro-fiber over a period of more than 3 h. By selecting low laser intensities optimized for spectral acquisition (3–6 mW laser power at the sample), we ensured that the observed Raman spectral shifts were due to applied mechanical stress and not caused by thermally-induced changes in the micro-fiber.

Borosilicate glass micropipettes (Corning®) with an outer diameter of 1 mm and an inner diameter of 0.55 mm were used together with a Narishige PP-830 pipette puller to create glass micro-needles with fine tip diameters $\leq 100 \mu\text{m}$. For the Hooke's law based calibration, we employed an optical lens system to determine the tip deflection of the flexible micro-needle. This was accomplished by using LED illumination of the micro-needle from the macroscopic end via an optical fiber and several lenses to project a magnified image of the coupled light exiting from

the fine tip of the micro-needle onto a computer-interfaced CCD camera (902DM2S; Watec Co. Ltd., Tsuruoka, Japan). The tip deflection was then measured with different tungsten weights suspended from the micro-needle. The overall calibration process included two steps: i) calibrating the tip deflection against the measured deflection on the computer screen using a micrometer, and ii) determining the tip deflection as a function of increasing mass suspended from the micro-needle.

Fig. 2a and b show a schematic representation of the calibration setup and a deflection/calibration curve used to obtain the spring constant of the flexible glass micro-needle, respectively. Images of the micro-needle tip were recorded before and after the flexible tip was displaced by micrometer. For calibration of the magnification optics, it was determined that 1 mm of actual displacement corresponded to 206 pixels on the CCD camera for all experiments, thus yielding a resolution of $4.85 \times 10^{-3} \text{ mm/pixel}$.

Tungsten wires with a diameter of $50 \mu\text{m}$ and of varying lengths, and thus varying masses, were used for the micro-needle calibration by loading them at the end of the fine tip. The position of the light spot exiting the illuminated micro-needle was determined before a weight was applied using the CCD camera and compared to that resulting from the deflection caused by the weight. The displacement in pixel units was determined by calculating the vertical distance that the light spot moved on the

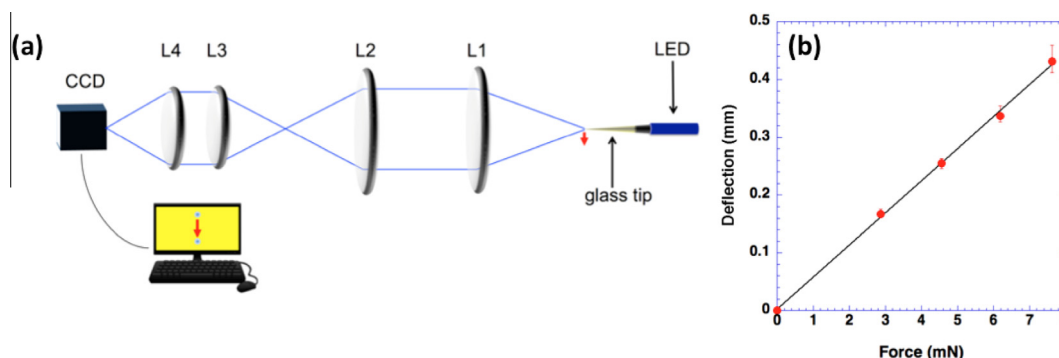


Fig. 2. (a) Schematic representation of the optical set-up for calibration. The glass needle is equipped with a light source. The light is propagating through a pair of converging lenses (L1, L2) for magnification. After a further magnification (L3, L4) the light spot image is projected onto a CCD camera and the resulting image computer processed. (b) Force-deflection curve of a flexible tip for calibration using tungsten wires as weights. Linear regression (black line) allows for determination of the spring constant from the calibration. The bar represents the full range of variation in the data for which the average deflection (four replicate measurements on one glass needle) was calculated.

computer screen upon loading due to the gravitational force. We defined the position of the micro-needle tip with and without the weight added for calibration. Due to the circular cross-section of the micro-needle tip, we assumed that the relative position of the tip is equivalent to the center of the light spot. For this purpose we performed line-scans across each image and plotted the intensity profiles. Each profile followed a Gaussian distribution and curve fitting was performed to determine the precise center of the spot. The gravitational force acting on the micro-needle tip was then calculated from $F_G = mg$ where m represents the mass of tungsten wire and $g = 9.82 \text{ m/s}^2$ is the gravitational constant. Four tungsten weights with increasing masses were used for the calibration and the resulting gravitational forces and mean displacements in pixels are shown in Fig. 2b. The force exerted on the tip [20] is given by $F_R = -k\Delta\chi$, where k is the spring constant of the micro-needle tip and $\Delta\chi$ is the displacement of the tip caused by gravity acting on the mass m . It is required that $F_R = -F_G$ and hence $k = mg/\Delta\chi$ and therefore the tip deflection is proportional to the applied mass. Using the values for m and $\Delta\chi$ shown in Fig. 2b, we obtained $k = 17.9 \pm 1.2 \text{ N/m}$. This value was used to determine the forces applied to the micro-fibers by displacement of the PZT.

Raman spectra were recorded by a dispersive confocal Raman spectrometer (Horiba XploRA). A green laser diode with a wavelength of 532 nm, a nominal output power of up to 25 mW and a spot size of approx. $1 \mu\text{m}$ was used as the excitation source. The Raman signal was detected by a silicon CCD detector and 90 scans were collected with an exposure time of 2 s. The spectral range varied from 500 to 4000 cm^{-1} with an instrumental spectral resolution of $1\text{--}2 \text{ cm}^{-1}/\text{pixel}$.

Replicate measurements (n) of glass needle deflection and micro-fiber stress-strain were performed four and seven times, respectively, and three replicate Raman shift measurements on each micro-fiber investigated. For each experimental data point, an average value was calculated for these replicates and plotted together with the full range of variation in the data as indicated in the respective figures.

The collagen/mineral micro-fibers were produced following a mineralization approach allowing for the formation of a bio-inspired nanostructure consisting of nano-apatite (Ap) crystals uniformly distributed in the bio-polymeric collagen matrix. This structure is endowed with chemical-physical features which are similar to those found in newly formed bone tissues [21,22]. The organic component, working as a matrix mediating the mineralization process, was type I collagen extracted from equine tendon. The mineral phase consisted of apatite nano-crystals doped with magnesium ions (Mg^{2+}) to obtain a ratio of Mg/Ca of approx. 5% mol. The presence of magnesium ions was found to improve apatite nucleation within the collagen fibrils [23]. This method enables the manufacture of hybrid composites with a wide range of compositions, i.e. 10 to 70 wt% of mineral phase relative to the polymeric matrix used in our experiments. Thermogravimetric

analysis (TGA) was performed to determine the amount of mineral content deposited in the collagen matrix [23] and transmission electron microscopy (TEM) and X-ray diffractometry of mineralized collagen have previously been performed to confirm the presence of apatite within the collagen fibrils [24]. To ensure the presence of apatite in the samples studied using our method, a detailed analysis of the mineralized micro-fibers was undertaken by using a focused ion beam to prepare a thin lamella from a 50% mineralized micro-fiber which was subsequently characterized by TEM and selected area electron diffraction (see [Supplementary Information, Fig. S11](#)). A structural comparison between the micro-fibers and the human bone revealed that the mineral phase was homogeneously incorporated within the micro-fibers. However, the morphology of the nanocrystals is somewhat different with regard to crystal diameter, elongation and orientation. We also imaged the micro-fibers by scanning electron microscopy (SEM) using a FEI-Sirion electron microscope (EM) and a 5 kV acceleration voltage. To compare the microstructure of the synthetic collagen/apatite composite with the ultrastructure of bone, we performed scanning TEM (STEM) using an aberration corrected JEOL 2200FS EM and a 200 kV acceleration voltage.

2.2. Experimental results

The micro-fiber elongation due to the external stress was determined by measuring the length of the micro-fiber when relaxed and strained as shown in Fig. 3. We applied equivalent stresses with a strain rate of $0.6\text{--}0.9\%/s$ where the stress is given by the applied force divided by the cross-sectional area of the micro-fiber. Assuming cylindrical geometry for the micro-fiber, the area was determined from $A = \pi r^2$ where r is the micro-fiber radius. Since the diameter is not always homogeneous along the entire length, it can be difficult to determine the equivalent stress values for the whole micro-fiber. In such cases, the stress is calculated only for a portion of the micro-fiber where the diameter is approximately homogeneous during an elongation of several micrometers and Raman spectra were recorded at these positions.

From the resulting stress-strain curves, we derived the Young's modulus E as a function of the degree of mineralization. Fig. 4a and b show a scanning electron micrograph of a single 50% mineralized fibril and the stress-strain curves of 0%, 50% and 70% mineralized collagen micro-fibers, respectively. We observed that the addition of apatite crystals in the collagen matrix significantly changes the mechanical response of the micro-fibers. Due to the limitations of the PZT displacement range, maximal strains of 6.4% could be realized for the non-mineralized collagen micro-fibers. For the 50% mineralized collagen, we observed rupture above approximately 6% strain. The presence of apatite crystals was enhancing the stiffness of the micro-fiber, but also reducing its elastic deformation range and thus its fracture toughness. This behavior was even more

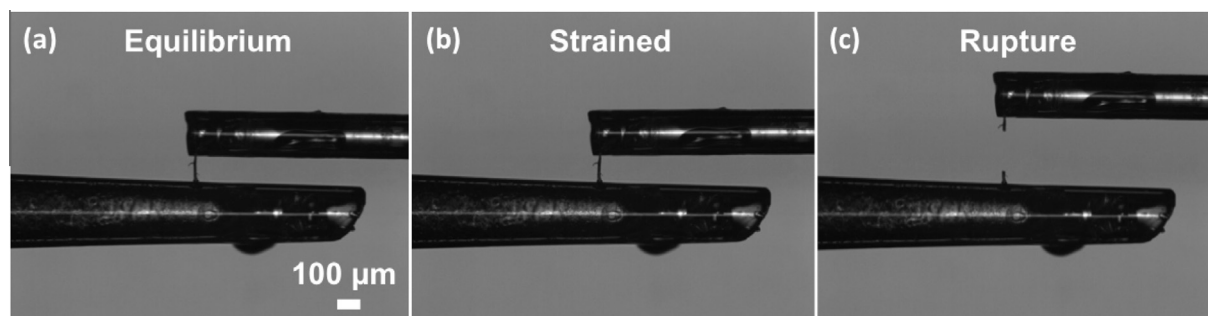


Fig. 3. Optical microscopy images of (a) relaxed, (b) strained and (c) ruptured collagen micro-fiber using the PZT device.

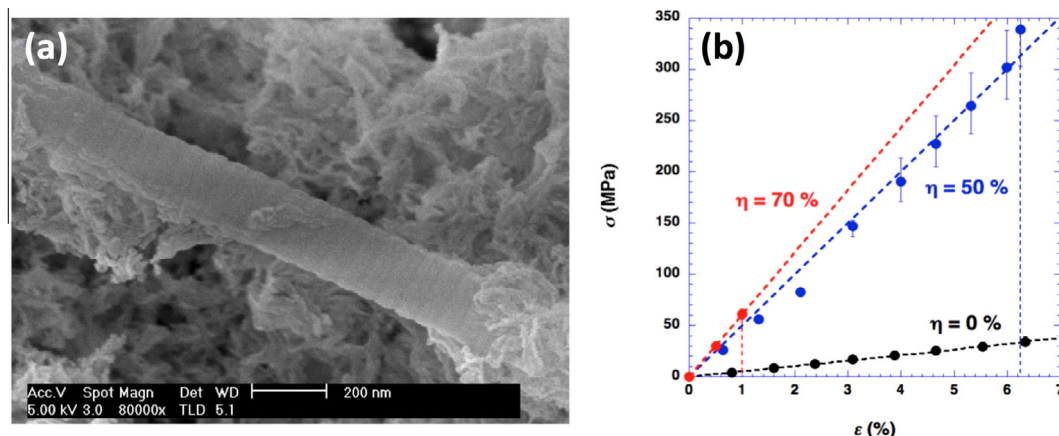


Fig. 4. (a) SEM image of 50% mineralized collagen fibril. (b) Stress-strain curves of non-mineralized (black), 50% mineralized (blue) and 70% mineralized (red) collagen micro-fibers with linear regression of the average stress values shown as dashed lines. Dashed vertical lines indicate maximal strain at micro-fiber rupture. σ refers to the stress (MPa), ϵ to the strain (%), and η to the amount of mineral content (wt%). The bar represents the full range of variation in the data for which the average stress (seven replicate measurements done on one or two micro-fibers) was calculated. (For interpretation of the references to colour in this figure legend, the reader is referred to the web version of this article.)

pronounced in the case of 70% mineralization where all investigated micro-fibers ruptured for strains above 1%.

Examples of Raman spectra for non-mineralized and mineralized collagen with all collagen/apatite Raman bands assigned (see Table 1) are displayed in Fig. 5. The spectra show all collagen bands at similar relative intensities and signal-to-noise ratios within the scanned spectral range and the phosphate-related band in the mineralized micro-fiber at 958 cm^{-1} . The good signal-to-noise ratio enabled a detailed investigation of the response of individual Raman bands to tensile stress.

Collagen micro-fibers with different mineral contents were subjected to uniaxial tensile stress using our custom-built device. Simultaneous Raman spectra were acquired to probe the molecular response to the applied stress. The micro-fibers were strained incrementally and Raman spectra were repeatedly recorded at each strain level. The fundamental difference between instrumental spectral resolution and precision in Raman band position assignment should be noted here. According to previously published reports [25,26], the position of a Raman band determined via curve fitting (assuming low-noise spectral data) can be assessed with sub-pixel resolution, and provides wavelength precision which is 10–30 times higher than the instrumental spectral resolution. As a result, Raman shifts of certain bands can be subsequently measured with a precision of approx. 0.05 cm^{-1} allowing for a detailed analysis of the response of characteristic Raman bands to stress. Whereas the non-mineralized micro-fibers showed no detectable shift of any of the collagen-related bands, we observed a clear shift of the proline and hydroxyproline related Raman bands as a function of strain, for example as shown in Fig. 6 for 0% and 50%

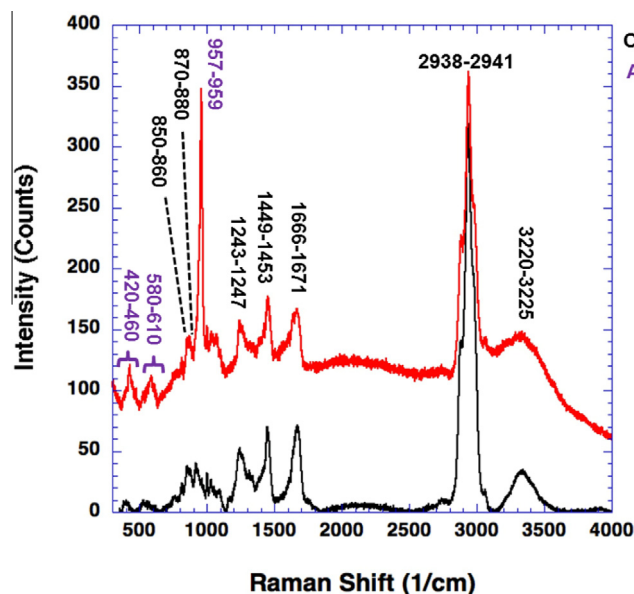


Fig. 5. Raman spectra of unstrained non-mineralized collagen (black) and 70% mineralized collagen (red) showing the characteristic Raman bands in accordance with Table 1. The presence of the apatite mineral is indicated by the ν_1 phosphorus-oxygen stretching mode. (For interpretation of the references to colour in this figure legend, the reader is referred to the web version of this article.)

Table 1
Characteristic collagen/apatite Raman bands [27,28].

Peak position (cm^{-1})	Assignment
420–460	ν_2 phosphate bending mode
570–620	ν_4 phosphate bending mode
850–860	Proline [$\nu(\text{CC})$, $\delta(\text{CCH})$]
870–880	Hydroxyproline [$\nu(\text{CC})$, $\delta(\text{CCH})$]
957–959	ν_1 phosphate (apatite)
1243–1246	Amide III
1449–1453	$\nu(\text{CH}_2\text{CH}_3)$ amino acid side chains
1666–1670	Amide I
2939–2942	$\nu(\text{CH}_2\text{CH}_3)$ amino acid side chains
3220–3225	$\nu(\text{OH})$ in water

ν – stretching mode, δ – bending mode.

mineralized collagen micro-fibers at different applied strain values. A detailed analysis of the Raman band shift was performed for all micro-fibers as a function degree of mineralization. A more detailed description of the Raman band evaluation procedure is provided in the Supplementary Information (see Fig. S12).

The proline/hydroxyproline Raman shift at increasing strain values becomes more prominent at higher values for η as shown in Fig. 7. For $\eta = 0\%$, the proline band did not show significant variations for strains up to values of 4.5%, while for 50% mineralization, a prominent Raman shift of -1.6 cm^{-1} could be observed for similar strain values. Previously, it has been reported that significant Raman shifts in non-mineralized collagen could only be observed for strain values of 17% and higher [18]. The Young's modulus – as determined from the stress-strain curves – shows a pronounced

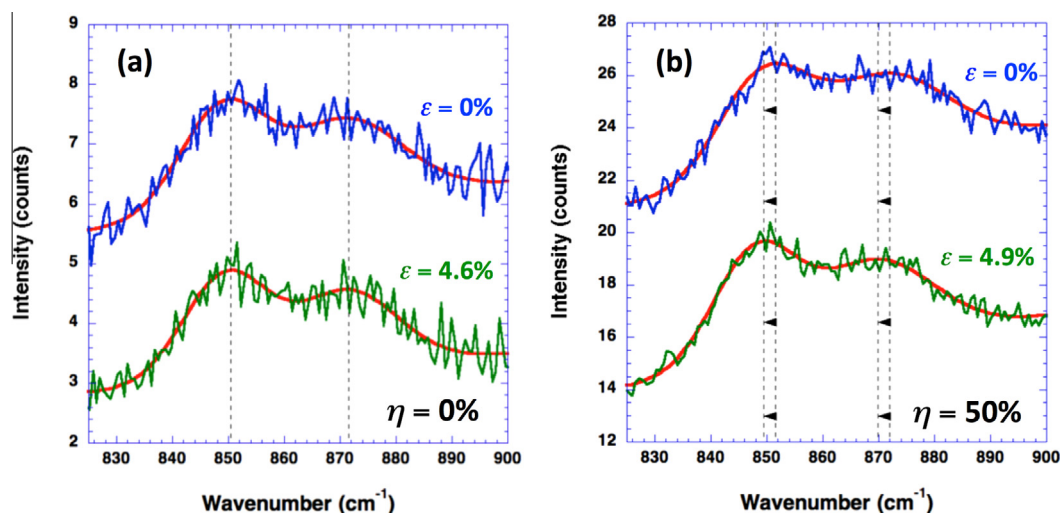


Fig. 6. Strain dependence of Raman shifts of the proline and hydroxyproline bands for (a) 0% and (b) 50% mineralized collagen. A comparison of the two respective Gaussian fits (red lines) shows a 1.8 cm^{-1} wavenumber shift for the strained mineralized collagen for both bands in this case. The blue and green lines represent the Raman spectra for unstrained and strained conditions in both samples. The value ε is the strain (%) and the value η is the amount of mineral content (wt%). (For interpretation of the references to colour in this figure legend, the reader is referred to the web version of this article.)

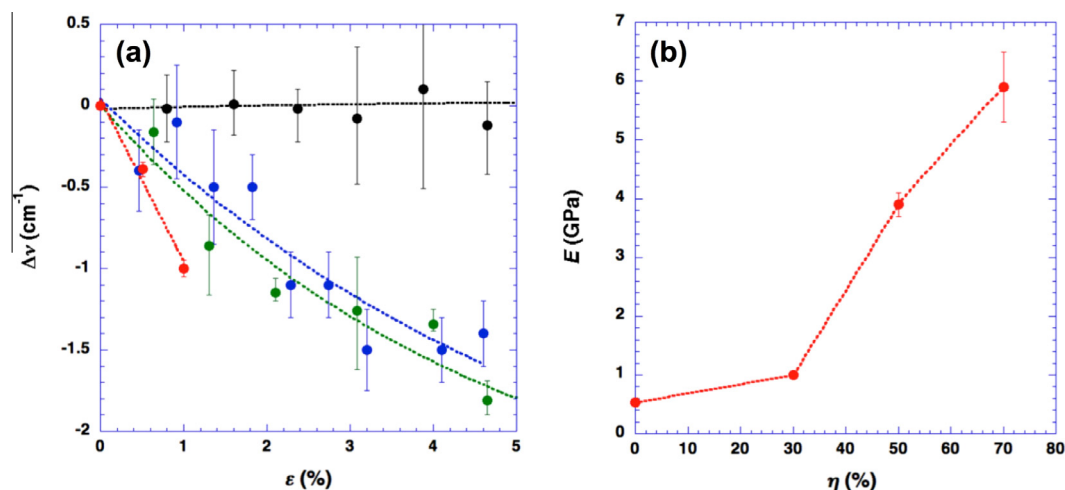


Fig. 7. (a) Average Raman shift of the proline band as a function of strain for 0% (black), 30% (blue), 50% (green) and 70% (red) mineral content of the micro-fibers. Dashed lines represent exponential fits to the data. (b) Average Young's modulus E (red) as a function of the degree of mineralization η . Dashed line is included to guide the reader's eye. The bars represent the full range of variation in the data (four replicate measurements on one or two micro-fibers) for which the average Raman band shift ($n = 3$) and Young's modulus ($n = 7$) were calculated. (For interpretation of the references to colour in this figure legend, the reader is referred to the web version of this article.)

increase for mineral content above 30% reaching 6 GPa in the case of 70% mineral content (see Fig. 7b).

2.3. Discussion

Our findings reveal a strong correlation between the molecular and the mechanical properties of collagen, and the crucial role of mineral crystals for load transfer into the collagen matrix. According to atomistic simulations performed by Nair et al. [29], the gap regions between tropo-collagen helices are more deformable and hence the overlap regions carry more stress in non-mineralized collagen. When apatite crystals form within the fibrils, the overlap regions become less deformable and the stress is transferred to the collagen molecules. Our interpretation of the correlation between mineralization and stress-strain response of the micro-fibers is summarized in Fig. 8. The schematic models in Fig. 8a and b show the staggered arrangement of the triple-helical collagen molecules found in collagen fibrils in the absence (Fig. 8a) and presence of

mineral nano-crystals (Fig. 8b, indicated in yellow). The presence of the mineral phase leads to an enhanced connectivity between the tropo-collagen molecules and hence an increased interlocking of fibrils. As a consequence, the presence of the mineral effectively alters the load transfer mechanism and hence the mechanical properties. In this context, the alignment of the apatite nanocrystals with respect to the collagen fibril orientation is expected to play an important role. The arrangement of the apatite nanocrystals in the context of the collagen fibers in human femur bone (Fig. 8c) can be observed in a STEM image of the apatite nanocrystals and the collagen fibrils, which are identifiable due to their characteristic D-banding. Note that the sample was not stained for contrast enhancement. There is a clear indication of a general alignment of the apatite nanocrystals with the long axes parallel to the orientation of the collagen fibrils. Previous reports on the stress-strain response of bone have highlighted the role of non-collagenous organics in the dissipation of energy [30,31]. In particular the possibility of stress relaxation via the reversible disruption



Fig. 8. Schematic illustrating the role of increased degree of mineralization in the enhanced stiffness of collagen. (a) Unloaded and loaded case of non-mineralized collagen showing the gap region between the triple collagen helices expanding. (b) Unloaded and loaded case for mineralized collagen (mineral phase in yellow) showing the mineral nanocrystals interlocking the triple helices. (c) Apatite crystals in the collagen matrix of human bone as observed by STEM. (For interpretation of the references to colour in this figure legend, the reader is referred to the web version of this article.)

of a largely homogeneous glue-like matrix of organic polymers such as polysaccharides has been suggested to explain the high toughness observed in bone [29].

The Young's modulus of bone has been reported to be approximately 20 GPa [32], which is about three times higher than our value for 70% mineralized collagen. This difference might be attributed to the absence of the non-collagenous component in our samples as well as the cross-linking between the collagen fibrils. However, a value of approximately 6 GPa, as found in our studies, is remarkably close to that of bone and despite the observed differences in the mineral microstructure, demonstrates the ability of the synthesis technique employed here to generate collagen/apatite composites with elastic properties similar to their natural counterpart.

It has previously been noted that mineral/collagen interactions may be a key factor in defining the characteristic hardness and fracture toughness of bone [30]. In particular, the stress release and energy dissipation pathways are determined by the nature of the interfaces between the apatite mineral and the tropo-collagen. The responsiveness of the proline/hydroxyproline bands to tensile stress can therefore provide valuable information regarding these interfaces.

The particular sensitivity of proline and hydroxyproline containing polypeptide sequences to external stress in the mineralized fibrils is important since both amino acids are known to stabilize the helical collagen structure. Our findings highlight that this interaction affects the mechanical response in the presence of apatite mineral and needs to be taken into account when preparing improved mineralized collagen tissue for bone replacement. For example, the collagen/apatite composite might be strengthened by increasing the proline and hydroxyproline composition of the polypeptide chains in the tissue. Current efforts focus on the use of computational simulations to determine the specific mechanism behind the molecular response to stress as revealed by the observed Raman frequency shift.

3. Summary

A novel custom-built electromechanical device combined with *in situ* Raman microscopy was used to study the molecular response of collagen micro-fibers with different amounts of apatite mineralization under tensile stress. We report that the presence of apatite crystals in the collagen triple helical matrix results in the enhancement of the elastic modulus of the micro-fibers, which is accompanied by a wavenumber decrease for the proline and hydroxyproline Raman bands with increasing strain. This is in contrast to non-mineralized collagen, where the elastic modulus is considerably lower and no significant dependence of the proline

Raman band on the applied stress could be detected. At levels of mineralization similar to those found in bone, the mechanical properties approach those of bone despite the absence of cross-linking in the collagen matrix. The observed systematic correlation between Young's modulus and proline Raman band shift is explained by a structural enhancement via molecular interlocking mediated by the mineral phase, which leads to an enhanced stiffness as well as sensitivity of the proline ring conformation to applied mechanical stress. We propose that a similar interlocking mechanism acts in natural bone and contributes significantly to its overall mechanical properties.

Acknowledgements

We acknowledge funding by the European Research Council in the framework of the SMILEY (FP7-NMP-2012-SMALL-6-310637) project and the Engineering and Physical Sciences Research Council (EP/I001514/1), and we gratefully acknowledge critical discussions with Natalie Reznikov and Jose-Manuel Delgado regarding the data interpretation.

Appendix A. Supplementary data

Supplementary data associated with this article can be found, in the online version, at <http://dx.doi.org/10.1016/j.actbio.2016.09.028>.

References

- [1] N. Nassif, F. Gobeaux, J. Seto, E. Belamie, P. Davidson, P. Panine, G. Mosser, P. Fratzl, M.M. Giraud-Guille, Self-assembled collagen-apatite matrix with bone-like hierarchy, *Chem. Mater.* 22 (2010) 3307.
- [2] A. Masic, L. Bertinetti, R. Schuetz, L. Galvis, N. Timofeeva, J.W.C. Dunlop, J. Seto, M.A. Hartmann, P. Fratzl, Observations of multiscale, stress-induced changes of collagen orientation in tendon by polarized Raman spectroscopy, *Biomacromolecules* 12 (2011) 3989.
- [3] J.D. Currey, The design of mineralised hard tissues for their mechanical functions, *J. Exp. Biol.* 202 (1999) 3285.
- [4] J.Y. Rho, L. Kuhn-Spearing, P. Zioupos, Mechanical properties and the hierarchical structure of bone, *Med. Eng. Phys.* 20 (1998) 92.
- [5] S. Weiner, W. Traub, H.D.J. Wagner, Lamellar bone: structure – function relations, *Struct. Biol.* 126 (1999) 241.
- [6] F. Hang, A.H. Barber, Nano-mechanical properties of individual mineralized collagen fibrils from bone tissue, *R. Soc. Interface* 8 (2011) 500.
- [7] D.A. Wahl, J.T. Czernuszka, Collagen-hydroxyapatite composites for hard tissue repair, *Eur. Cells Mater.* 11 (2006) 43.
- [8] D.A.D. Parry, The molecular fibrillar structure of collagen and its relationship to the mechanical properties of connective tissue, *Biophys. Chem.* 29 (1988) 195.
- [9] K.E. Kadler, D. Holmes, J. Trotter, J. Chapman, Collagen fibrils in vitro grow from pointed tips in the C- to N-terminal direction, *Biochem. J.* 316 (1996) 1.
- [10] Y. Tang, R. Ballarín, M.J. Buehler, S.J. Eppell, Deformation micromechanisms of collagen fibrils under uniaxial tension, *J. R. Soc. Interface* 7 (2009) 839.
- [11] P. Fratzl (Ed.), *Collagen: Structure and Mechanics*, Springer-Verlag, Berlin, 2008.

- [12] P. Fratzl, H.S. Gupta, E.P. Paschalis, P. Roschger, Structure and mechanical quality of the collagen–mineral nano-composite in bone, *J. Mater. Chem.* 14 (2004) 2115.
- [13] T. Hirschfeld, B. Chase, FT-Raman spectroscopy: development and justification, *Appl. Spectrosc.* 40 (1986) 133.
- [14] E. Gentleman, A.N. Lay, D.A. Dickerson, E.A. Nauman, G.A. Livesay, K.C. Dee, Mechanical characterization of collagen fibers and scaffolds for tissue engineering, *Biomater* 24 (2003) 3805.
- [15] Y.N. Wang, C. Galiotis, D.L. Bader, Determination of molecular changes in soft tissues under strain using laser Raman microscopy, *J. Biomech.* 33 (2000) 483.
- [16] S.J. Eppell, B.N. Smith, H. Kahn, R. Ballarini, Nano measurements with micro-devices: mechanical properties of hydrated collagen fibrils, *J. R. Soc. Interface* 3 (2006) 117.
- [17] M.P.E. Wegner, L. Bozec, M.A. Horton, P. Mesquida, Mechanical properties of collagen fibrils, *Biophys. J.* 93 (2007) 1255.
- [18] M. Gasior-Glogowska, M. Komorowska, J. Hanuza, M. Ptak, M. Kobielar, Structural alteration of collagen fibres – spectroscopic and mechanical studies, *Acta Bioeng. Biomech.* 12 (2010) 55.
- [19] M. Gasior-Glogowska, M. Komorowska, J. Hanuza, M. Maczka, R. Bedziński, M. Kobielar, *J. Mech. Behav. Biomed. Mater.* 18 (2013) 240.
- [20] R. Hooke, *Lectures de Potentia Restitutiva or Of Spring, Explaining the Power of Springing Bodies*, London, Printed for John Martyn, 1678.
- [21] A. Tampieri, G. Celotti, E. Landi, M. Sandri, N. Roveri, G. Falini, *J. Biomed. Mater. Res. Part A* 67A (2003) 618.
- [22] A. Tampieri, M. Sandri, E. Landi, S. Sprio, F. Valentini, A.L. Boskey, Synthetic bio-mineralization yielding HA/collagen hybrid composite, *Adv. Appl. Ceram.* 107 (5) (2008) 298.
- [23] A. Tampieri, S. Sprio, M. Sandri, F. Valentini, Biologically inspired synthesis of bone-like composite: self-assembled collagen fibers/hydroxyapatite nanocrystals, *Trends Biotechnol.* 29 (2011) 526.
- [24] S. Sprio, M. Sandri, S. Panseri, C. Cunha, A. Tampieri, Hybrid scaffolds for tissue regeneration: chemotaxis and physical confinement as sources of biomimesis, *J. Nanomater.* 2012 (2012). Article ID 418281.
- [25] E.S. Izraeli, J.W. Harris, O. Navon, Raman barometry of diamond formation, *Earth Planet. Sci. Lett.* 173 (1999) 351.
- [26] S. Fukura, T. Mizukami, S. Odake, H. Kagi, Factors determining the stability, resolution, and precision of a conventional Raman spectrometer, *Appl. Spectrosc.* 60 (8) (2006) 946.
- [27] J.J. Cárcamo, A.E. Aliaga, R.E. Clavijo, M.R. Brânes, M.M. Campos-Valette, Raman study of the shockwave effect on collagens, *Spectrochim. Acta A* 86 (2012) 360.
- [28] G.S. Mandair, M.D. Morris, Contributions of Raman spectroscopy to the understanding of bone strength, *Bonekey Rep.* 4 (2015) 620.
- [29] A.K. Nair, A. Gautieri, S.W. Chang, M.J. Buehler, Molecular mechanics of mineralized collagen fibrils in bone, *Nat. Commun.* 4 (2013) 1724.
- [30] G.E. Fantner, T. Hassenkam, J.H. Kindt, J.C. Weaver, H. Birkendal, L. Pechenik, J. A. Cutroni, G.A.G. Cidade, G.D. Stucky, D.E. Morse, P.K. Hansma, Sacrificial bonds and hidden length dissipate energy as mineralized fibrils separate during bone fracture, *Nat. Mater.* 4 (2005) 612.
- [31] R. Ping Hoo, P. Fratzl, J.E. Daniels, J.W.C. Dunlop, V. Honkimäki, M. Hoffman, Cooperation of length scales and orientations in the deformation of bovine bone, *Acta Biomater.* 7 (2011) 2943.
- [32] J.Y. Rho, R.B. Ashman, C.H. Turner, Young's modulus of trabecular and cortical bone material: ultrasonic and microtensile measurements, *J. Biomech.* 26 (1993) 111.